

# Relative optical wavefront measurement in displacement measuring interferometer systems with sub-nm precision

Arjan J. H. Meskers,<sup>1,\*</sup> Dirk Voigt,<sup>2</sup> and Jo W. Spronck<sup>1</sup>

<sup>1</sup>*Delft University of Technology, department of Precision and Microsystems Engineering, Mekelweg 2, 2628CD Delft, the Netherlands*

<sup>2</sup>*VSL Dutch Metrology Institute, Thijssseweg 11, 2629 JA Delft, The Netherlands*

*\*a.j.h.meskers@tudelft.nl*

**Abstract:** Many error sources can affect the accuracy of displacement measuring interferometer systems. In heterodyne interferometry two laser source frequencies constitute the finally detected wavefront. When the wavefronts of these source frequencies are non-ideal and one of them walks off the detector, the shape of the detected wavefront will vary. This leads to a change in measured phase at the detector resulting in increased measurement uncertainty. A new wavefront measurement tool described in this publication measures the relative phase difference between the two wavefronts of the two source frequencies of a coaxial heterodyne laser source as used in commercial heterodyne interferometer systems. The proposed measurement method uses standard commercial optics and operates with the same phase measurement equipment that is normally used for heterodyne displacement interferometry. In the presented method a bare tip of a multimode fiber represents the receiving detection aperture and is used for locally sampling the wavefront during a line scan. The difference in phase between the beating frequency of the scanning fiber and a reference beating frequency that results from integration over the entire beam, is used for the reconstruction of the wavefront. The method shows to have a phase resolution in the order of  $\sim 25$  pm or  $\sim \lambda/25000$  for  $\lambda$  632.8 nm, and a spatial resolution of  $\sim 60$   $\mu$ m at a repeatability better than 1 nm over one week.

©2013 Optical Society of America

**OCIS codes:** (120.0120) Instrumentation, measurement and metrology; (120.3180) Interference; (120.3930) Metrological Instrumentation; (120.4570) Optical design instruments (120.4630) Optical inspection; (120.4640) Optical instruments; (120.4820); Optical systems; (120.5050) Phase measurement; (060.2840) Heterodyne.

---

## References and links

1. N. Bobroff, "Recent advances in displacement measuring interferometry," *Meas. Sci. Technol.* **4**(9), 907–926 (1993).
2. F. C. Demarest, "High-resolution, high-speed, low data age uncertainty, heterodyne displacement measuring interferometer electronics," *Meas. Sci. Technol.* **9**(7), 1024 (1998).
3. A. Abramovici, W. E. Althouse, R. W. P. Drever, Y. Gürsel, S. Kawamura, F. J. Raab, D. Shoemaker, L. Sievers, R. E. Spero, K. S. Thorne, R. E. Vogt, R. Weiss, S. E. Whitcomb, and M. E. Zucker, "LIGO: The Laser Interferometer Gravitational-Wave Observatory," *Science* **256**(5055), 325–333 (1992).
4. K. Danzmann and L. I. S. A. team, "LISA: laser interferometer space antenna for gravitational wave measurements," *Class. Quantum Gravity* **13**(11A), A247–A250 (1996).
5. T. Schuldt, M. Gohlke, D. Weise, U. Johann, A. Peters, and C. Braxmaier, "Picometer and nanoradian optical heterodyne interferometry for translation and tilt metrology of the LISA gravitational reference sensor," *Class. Quantum Gravity* **26**(8), 085008 (2009).
6. H.-J. Butt, B. Cappella, and M. Kappl, "Force measurements with the atomic force microscope: Technique, interpretation and applications," *Surf. Sci. Rep.* **59**(1-6), 1–152 (2005).

7. J. Leach, M. J. Padgett, S. M. Barnett, S. Franke-Arnold, and J. Courtial, "Measuring the Orbital Angular Momentum of a Single Photon," *Phys. Rev. Lett.* **88**(25), 257901 (2002).
8. P. de Groot, J. Biegen, J. Clark, X. C. de Lega, and D. Grigg, "Optical interferometry for measurement of the geometric dimensions of industrial parts," *Appl. Opt.* **41**(19), 3853–3860 (2002).
9. S. J. A. G. Cosijns, H. Haitjema, and P. H. J. Schellekens, "Modeling and verifying non-linearities in heterodyne displacement interferometry," *Precis. Eng.* **26**(4), 448–455 (2002).
10. W. Hou and G. Wilkening, "Investigation and compensation of the nonlinearity of heterodyne interferometers," *Precis. Eng.* **14**(2), 91–98 (1992).
11. J. M. De Freitas and M. A. Player, "Polarization effects in heterodyne interferometry," *J. Mod. Opt.* **42**(9), 1875–1899 (1995).
12. K. N. Joo, J. D. Ellis, E. S. Buice, J. W. Spronck, and R. H. Schmidt, "High resolution heterodyne interferometer without detectable periodic nonlinearity," *Opt. Express* **18**(2), 1159–1165 (2010).
13. J. D. Ellis, A. J. H. Meskers, J. W. Spronck, and R. H. Munnig Schmidt, "Fiber-coupled displacement interferometry without periodic nonlinearity," *Opt. Lett.* **36**(18), 3584–3586 (2011).
14. G. Mana, "Diffraction Effects in Optical Interferometers Illuminated by Laser Sources," *Metrologia* **26**(2), 87–93 (1989).
15. K. Dorenwendt and G. Bönsch, "Über den Einfluß der Beugung auf die interferentielle Längenmessung," *Metrologia* **12**(2), 57–60 (1976).
16. A. Chernyshov, U. Sterr, F. Riehle, J. Helmcke, and J. Pfund, "Calibration of a Shack-Hartmann sensor for absolute measurements of wavefronts," *Appl. Opt.* **44**(30), 6419–6425 (2005).
17. A. F. Brooks, T. L. Kelly, P. J. Veitch, and J. Munch, "Ultra-sensitive wavefront measurement using a Hartmann sensor," *Opt. Express* **15**(16), 10370–10375 (2007).
18. H. Medeck, E. Tejn, K. A. Goldberg, and J. Bokor, "Phase-shifting point diffraction interferometer," *Opt. Lett.* **21**(19), 1526–1528 (1996).
19. G. R. Brady, M. Guizar-Sicairos, and J. R. Fienup, "Optical wavefront measurement using phase retrieval with transverse translation diversity," *Opt. Express* **17**(2), 624–639 (2009).

## 1. Introduction

Laser interferometry is applied for a wide range of measurement applications in the fields of high precision position sensing: measuring displacements of precision stages [1,2], gravitational wave detection in the LIGO [3] and LISA [4,5] projects, atomic force microscopy [6] and measuring orbital angular momentum of photons [7]. It is also often used for calibration of other measurement tools [8] such as capacitive sensors, inductive sensors, and optical encoders. In the field of positioning metrology it is possible to measure displacements with an uncertainty of less than a nanometer by means of optical interferometry. Heterodyne interferometry is a measurement method that can obtain sub-nm displacement uncertainty over a large dynamic range because of a high signal-to-noise ratio phase measurement. A number of error sources affect the measurement uncertainty: frequency stability of the laser source, refractive index variations in the measurement environment and optical components, system alignment [9] and periodic nonlinearity in the phase measurement [10,11]. Employment of laser stabilization and conditioning of the measurement environment can improve the obtained uncertainty. However, periodic nonlinearity in the measurand is difficult to eliminate because it arises from a combination of error sources [9,10]. Periodic nonlinearity plays an important role in sub-nm displacement uncertainty, recent research reports interferometer measurements without periodic nonlinearity [12,13]. Though some of the error sources can be eliminated or reduced such as the alignment related Cosine error and the Abbé error, there are still error sources in the system present that will be inherent to an interferometer system. Since these are optical systems it is for example important to understand how the optical wavefront behavior [14,15] can add to measurement uncertainty. Wavefront behavior in combination with beam walkoff is one of the error sources that cannot be eliminated when dealing with a multiple degrees of freedom (DOF) target. Target tilt will cause the measurement beam to reflect off the target under an angle and will show transverse displacement (i.e. beam walkoff) at the detector as illustrated in Fig. 1.

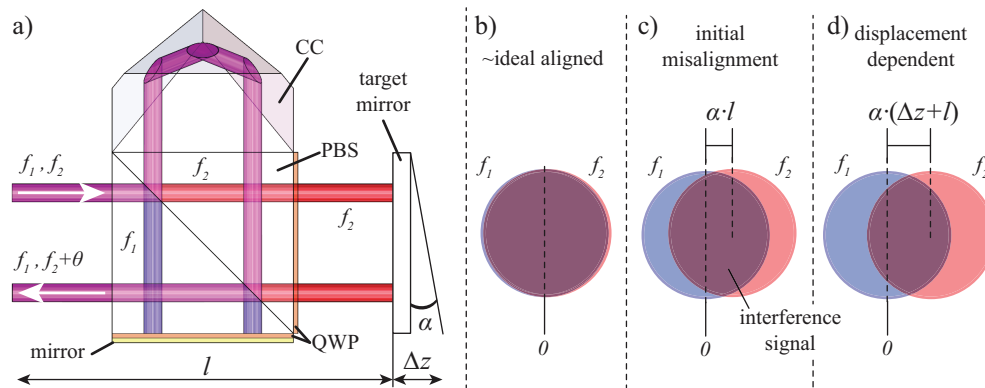


Fig. 1. System alignment and beam walkoff: a) ideal aligned single DOF heterodyne interferometer where reference and measurement beams ~fully overlap. Beam walkoff depends on target tilt  $\alpha$ , target displacement  $\Delta z$  and distance  $l$  between the target mirror and photodetector. Blue denotes the reference frequency  $f_1$  and red the measurement frequency  $f_2$ , b) ideal aligned system, c) initial misalignment due to target tilt  $\alpha$  and distance  $l$ , d) displacement dependent walkoff due to target displacement  $\Delta z$  in combination with  $\alpha$  and  $l$ .

More detailed investigation in wavefront quality in relation to beam walkoff and the integration area of the photodetector are therefore of importance in sub-nm displacement interferometry. In Fig. 1 a single DOF heterodyne interferometer is shown, fed by a coaxial beam containing two orthogonal-oriented linear polarized frequencies ( $f_1$  and  $f_2$ ) that have a constant frequency offset. A polarized beam splitter splits the two frequency components into a reference beam  $f_1$  and a measurement beam  $f_2$ . When ideally aligned both beams/frequencies fully overlap see Fig. 1(b), and create an interference signal at the overlapping area. When the target mirror tilts or misalignment occurs, beam walkoff takes place, see Fig. 1(c) and 1(d). In that situation the (red) measurement beam ‘walks off’ the (blue) reference beam which stays in place.

Wavefront deformations consist of phase differences throughout the cross-section of a laser beam and are caused by: a) the laser source, b) refractive index variations and c) reflective surfaces. Such wavefront deformations can be multiple nanometers large and are potentially a problem when sub-nm displacement uncertainty is to be obtained.

An ideal wavefront for optical metrology purposes is mostly defined as being ‘flat’ (i.e. having zero curvature); unfortunately every wavefront has one or more curvatures and is thus non-ideal. The non-ideal wavefronts of a (blue) reference- and (red) measurement beam in Fig. 2, are shown with exemplary sinusoidal shape deformations. In the situation *without walkoff* the overlapping wavefronts interfere over the full width of the photodetector. The resulting interference wavefront (purple) consists of the relative difference between the blue and red wavefront, the wavefront of the measured beating frequency is therefore a relative wavefront based upon the individual wavefront shapes of  $f_1$  and  $f_2$ . The horizontal dotted line denotes the phase integral of the interference signal. In the situation *with walkoff*, one wavefront shifts relative to the other resulting in a new wavefront shape of the interference signal, this also leads to a different phase integral. Comparing the obtained phase integrals of the two situations shows a phase difference  $\Delta\theta$ . In displacement interferometry the measured phase is multiplied by the wavelength of the source light to obtain target displacement. The  $\Delta\theta$  in the illustrated case therefore represents the displacement uncertainty caused by beam walkoff in combination with the non-ideal shaped wavefronts of  $f_1$  and  $f_2$ . Beside a change in the phase integral, beam walkoff also causes the signal strength of the interference signal to vary due to a change in the amount of overlap between the two beams.

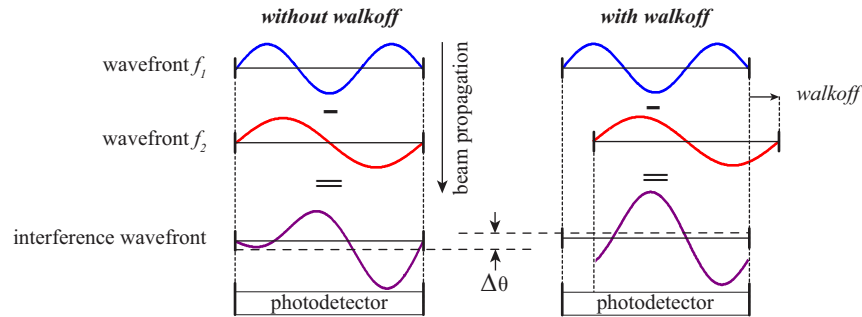


Fig. 2. Two measurements with non-ideal wavefronts: one *without walkoff* and *with walkoff*. The vertical axis shows the incoming wavefronts of the source frequencies that interfere and create the wavefront of the beat frequency were they overlap. Our heterodyne phase measurement signal retrieves a relative wavefront that consists of the wavefront differences between the wavefronts of  $f_1$  and  $f_2$ . The horizontal axis represents the diameter of the photodetector that integrates the phase of the incoming relative wavefront over its surface area. Beam walkoff results in a different phase integration compared to the situation without walkoff, the phase difference  $\Delta\theta$  is falsely interpreted as target displacement.

The main group of wavefront sensors is based upon the ‘Shack Hartmann’ principle, having a micro lens array that focuses onto a CCD. This method is able to measure the absolute wavefront topology of the whole cross-section of a beam in a single measurement but is sensitive for tip/tilt alignment. In this group of sensors a trade-off is seen between high phase resolution versus high spatial resolution which is limited by the size of the lenslet-array and the number of lenses. The phase resolution that can be obtained with these sensors ranges  $\lambda/100$  for an Ø6 mm beam diameter to  $\lambda/500$  for Ø1 mm at  $\lambda$  632.8 nm [16]. More recent research [17] showed measurement sensitivity up to  $\lambda/15500$  at  $\lambda$  820 nm, though the spatial resolution is again limited by a 30x30 lenslet-array over 12.5x12.5 mm. Phase shifting interferometers [18] measure with the same order of phase resolution and beam diameters but offer higher spatial resolution, limited by the CCD. Another method worth mentioning [19] is based upon phase retrieval. It samples the wavefront at different locations using a small moving subaperture while measuring intensity distributions with a CCD. The use of a small movable subaperture for wavefront sampling shows some resemblance with the method proposed in this publication.

The Shack Hartmann and point diffraction methods are relatively easy to implement as measurement tools for wavefront evaluation within existing systems but they are unable to combine high spatial resolution measurements at high phase resolution and large measurement areas simultaneously, using the same hardware.

In this article we describe a new and easy to implement measurement tool that uses standard commercial optics and phase measurement equipment that is normally used for heterodyne displacement interferometry. The method allows for varying the size of the measurement area and the phase resolution without the need for changing hardware and it enables to measure relative wavefront differences before as well as after an interferometer. The strength of our method we consider the simultaneous accessibility to both high phase and spatial resolution. Considering best possible resolution in either phase or spatial DOF alone, the state-of-the art is set by other approaches. Optimal choice in measurement concept will depend on more specific application needs.

## 2. Wavefront measurement system

*Note: The two lasers used for demonstrating the wavefront measurement method have in the past been opened during which components were removed and reinstalled. The wavefronts shown in this publication are due to the history of the lasers thus not representative for the wavefront quality of two properly used identical lasers. Also, the reason for measuring these*

two laser sources is NOT to evaluate the performance of the two lasers with respect to each other but only to demonstrate the wavefront measurement method.

The aim of the described wavefront measurement system is to demonstrate that it can measure the wavefront of an interference signal created from a heterodyne coaxial beam, enabling further investigation related to beam walkoff. The wavefronts of two laser sources have been measured (without interferometer optics in the system): the first laser is a Zeeman type laser from Agilent, type 5517D (i.e. *laser 1*) and the second laser is an AOM (Acousto Optic Modulator) laser from Zygo, type Axiom 2/20 (i.e. *laser 2*), both have Ø6 mm beams. The beating frequencies are ~4 MHz and ~20 MHz for respectively *laser 1* and *laser 2*.

The first component of the wavefront measurement system, Fig. 3, is a 45° polarizer creating interference between the two source frequencies. An 8% pellicle beam sampler (pbs) samples a reference signal that is equal to the beat frequency. A pellicle type beam sampler is preferred because of its low amount of refraction (i.e. 2 µm membrane thickness). The reference signal is coupled into a multimode fiber (core ~Ø1 mm) and is transported to a phase measurement board. By sampling of the entire beam the total wavefront is integrated within the reference beating frequency. A multimode step index optical fiber with a core diameter of 62.5 µm functions as the transversally scanned measurement probe aperture. The light coupled into this measurement fiber is only a fraction of the total optical power (~0.4 nW with *laser 1* and ~0.6 nW with *laser 2*) and consists of only the collinear radiation that is in front of the fiber; there is no light coupled into the fiber using lenses or other aids. The phase integration surface is thus equal to the fiber its core diameter. The measurement fiber is attached to a single DOF automated translation stage performing a continuous velocity displacement along the x-axis. The automated stage itself is located on top of a manually operated single DOF translation stage for displacement along the y-axis, see Fig. 4, enabling scanning through the coaxial beam at different elevations for 3D wavefront reconstruction.

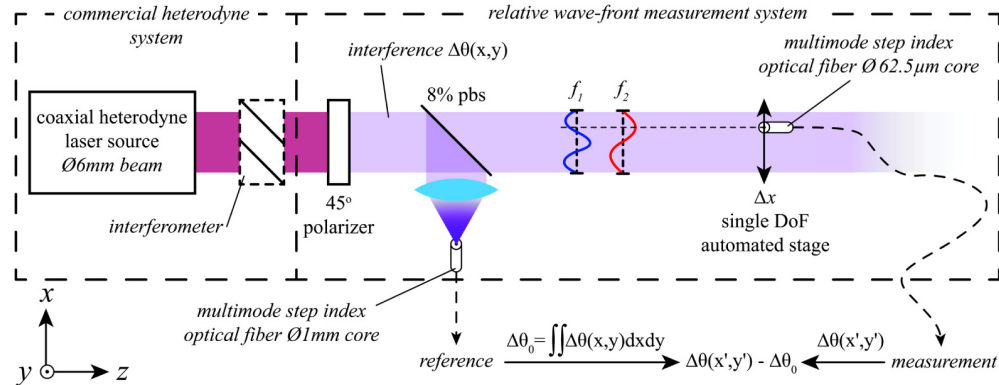


Fig. 3. Schematic overview of the measurement setup. An optionally inserted interferometer assembly is indicated. Such configuration should allow investigation of wavefront distortions as caused by the additional optical system. After exiting the heterodyne system the coaxial heterodyne beam passes a polarizer at 45° creating the interference signal, an 8% pellicle beam sampler (pbs) samples and integrates the interference signal over the entire beam to serve as a reference signal. An Ø62.5 µm multimode fiber measures locally the beating signal which is compared to the reference beating signal, resulting in phase changes  $\Delta\theta$  over the cross section of the beam when the wavefront is non-ideal i.e. deformed.

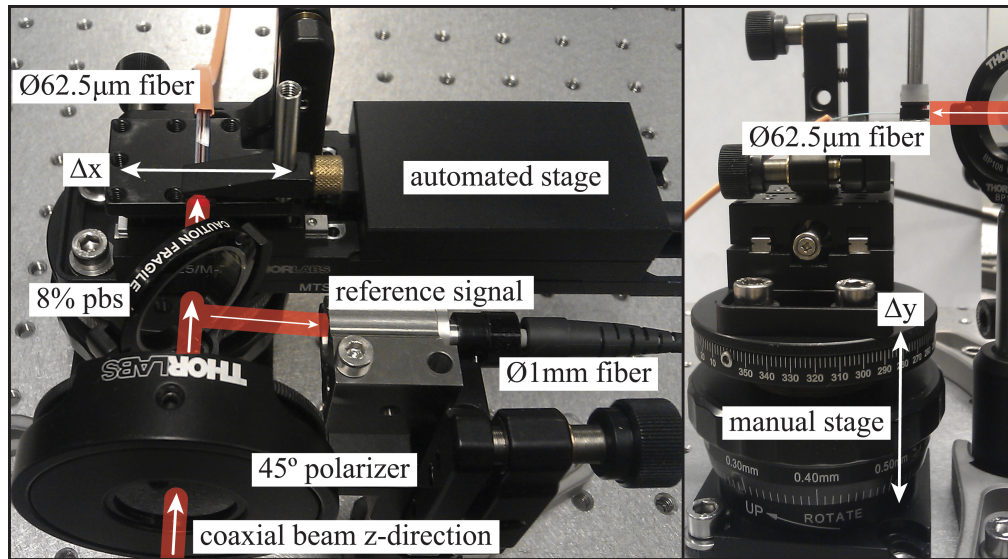


Fig. 4. The wavefront measurement system illustrated in Fig. 3, build in the lab. The left image shows the coaxial heterodyne beam coming in from the lower left passing a polarizer at 45°, then propagating through the 8% pbs (creating a reference signal) and finally reaching the multimode fiber on the automated stage. The right image shows more clearly the manual vertical y-displacement stage with the automated stage on top of it.

### 3. Relative wavefront measurements

The measurement method is demonstrated using a coherent coaxial heterodyne laser source without an optical interferometer present in the system. Optical system components and the air refractive index do not affect the measurement since the optical pathways for both frequencies are identical: if the wavefront of one frequency is disturbed the wavefront of the other frequency will be equally affected; resulting in no relative changes. This makes it possible to perform high resolution measurements even in an air environment.

When the Ø62.5 µm measurement fiber is at standstill at any location within the beam, the frequency of the measured interference signal is equal to the reference interference frequency that is integrated over the entire beam. When the measurement fiber traverses perpendicular through the beam it measures a beat frequency equal to the reference beat frequency but with a phase addition  $\Delta\theta$  as a function of the transverse horizontal 'x' position (when there exist relative differences between the wavefronts of  $f_1$  and  $f_2$ ), see Fig. 3. The measured phase  $\Delta\theta$  is then multiplied by the source wavelength resulting in a wavefront expressed in meters. An advantage of this optical phase measurement method over other methods is that it is not an intensity distribution measurement over a CCD but a frequency measurement of the interference signal and thereby resulting in higher noise suppression.

Each measurement consists of a line scan as the multimode fiber traverses at continuous velocity through the coaxial beam. All measurements are performed in an air environment at room temperature.

The applied phase-measurement equipment (Agilent N1225A) is normally used for heterodyne displacement interferometry and has a phase resolution of 0.6 nm with a max. buffer size of 700k data-points. This measurement board uses a 'leap frog' phase measurement technique that fits an internally generated sine wave according the measured beating frequency, obtaining high sensitivity and noise immunity. The board continuously samples and integrates phase over time at several MHz while allowing the user to download samples at a different rate, anywhere between ~610 Hz and ~62.5 kHz. All data used for this publication is sampled at 5.58 kHz, i.e. sampling period  $\tau_0 = 180 \mu\text{s}$ .



The repeatability of a measurement is defined as the closeness of the agreement between the results of successive measurements of the same measurand carried out under the same conditions of measurement. The repeatability is calculated by overlaying and subtraction of two successive line scans under the same measurement conditions and taking the root-mean-squared-value (RMS) of the difference between these two scans. The repeatability after 5 minutes is on the order of 0.8 nm and after a week 0.82 nm. These results show that the measurement method has a high repeatability and it also shows that the laser source has a high relative wavefront stability between the wavefronts of frequency  $f_1$  and  $f_2$ . This measurement method could therefore also be used as a tool to check for the relative wavefront stability of a coaxial heterodyne laser source.

The wavefront to be studied is sampled over  $\varnothing 62.5 \mu\text{m}$  by a multimode step index optical fiber. The obtained spatial resolution is currently limited by this dimension since it is not possible to distinguish between detection of a homogenous phase distribution or a gradient. However, when applying phase-deconvolution the spatial resolution can be further increased.

The phase-resolution of the current setup is limited by the amount of noise. An Allan deviation is used to find an optimal data averaging level where the noise presence is the lowest, indicating the maximum obtainable measurement resolution of the system. The Allan deviation typically shows an upswing at larger integration times which means averaging over more data points does not improve the measurement because drift has occurred. Figure 5 shows the results from a measurement in a static system. For this system an optimum can be found when the measurement signal is integrated over  $\sim 90$  ms corresponding to 500 samples (i.e.  $\tau_0 \times 500$ ), obtaining a resolution of  $\sim 25$  pm or  $\sim \lambda/25000$ . Shorter time integration shows an increased level of stochastic noise while longer time integration suffers from noise due to drift. It is important to note that this obtained performance highly depends on the used phase measurement equipment.

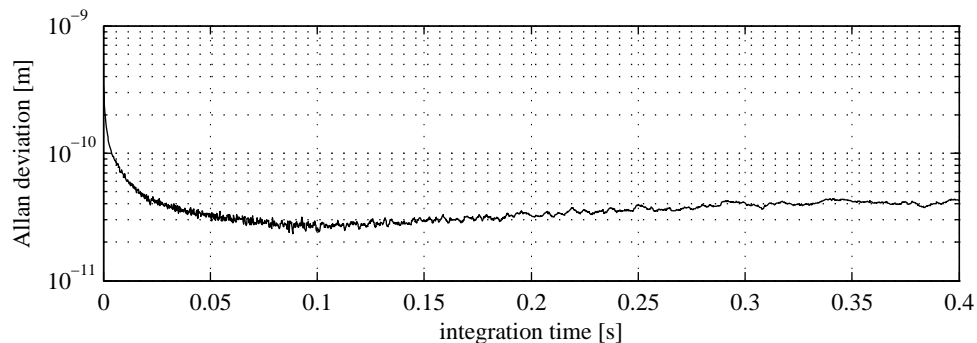


Fig. 5. Allan deviation plot showing an optimum at a sample integration period of 90ms, i.e. averaging over  $\sim 500$  data samples, at this location the noise presence is the lowest and a resolution of  $\sim 25$ pm (i.e.  $\sim \lambda/25000$ ) is obtained. From this graph we can also conclude that sub-nm resolution is still obtained when measuring at higher sampling rates.

#### 4. Results

This section is meant for investigating the correctness of the obtained wavefronts and to see what the first order influence is when a standard detector with a large measurement area is used instead of the relatively small core of a multimode fiber.

Figure 5 shows two line scans taken through the middle of the coaxial beams of the two lasers. The left graph shows the cross-section of the interference signal its wavefront from *laser 1*. Its shape can be explained by a Quarter Wave Plate (QWP) that is used for transforming the left- and right circular polarized output frequencies of a Zeeman type laser into two orthogonally oriented linear polarized frequencies. Tilting this plate prevents back reflections into the laser-cavity destabilizing lasing operation. Internal reflections within the

plate combined with polarization preference due to the tilt could be the source of the wave-like shape over a single axis.

The graph at the right of Fig. 6 originates from *laser 2*, an AOM type laser where the heterodyne frequency is generated by means of an AOM. The zero-order and the first-order modes from the AOM are made coaxial using a rotated wedge that compensates for the exit-angle of the first-order mode. The tilted wavefront could be the result of misalignment between the AOM and this wedge, the sloped curve seen in the graph corresponds with the rotation-axis of the wedge.

Both interference signal wavefront shapes can be justified together with the magnitude of deformation, it can therefore be assumed the measurement method measures correct.

At first sight these wavefront shapes do not seem suitable to be used for low uncertainty displacement measurements, they can be compensated however by using a larger measurement aperture and thereby increasing the phase integration area. Figure 7 shows what happens to a wavefront profile when measuring with an aperture of Ø11 mm (standard size Agilent remote receiver lens) instead of Ø62.5  $\mu\text{m}$ . Over a width of 6 mm at the center of the line-scans it can be seen that the deformations in both profiles are to a high degree minimized. For *laser 1* the error occurs mostly in the periphery of the beam, the irradiance-weighted phase measured from the entire beam is little affected by the small error signal at the periphery. *Laser 1* therefore allows for almost full beam walkoff and still obtains sub-nm uncertainty, *laser 2* allows for  $\pm 2$  mm beam walkoff when aiming for sub-nm uncertainty.

Figure 8 shows a 3D wavefront reconstruction consisting of multiple measurements. Between subsequent line-scans along the x-axis using the automated stage a displacement of 100  $\mu\text{m}$  is applied in the y-direction using the manual stage, see Fig. 4.

To exclude measuring artifacts caused by the optical components themselves, the measurement components have been relocated, tilted and if possible rotated between several test-measurements, no notable effects were observed. Also possible periodic displacement errors originating from the automated stage are excluded by scanning at different velocities forth- and back at different locations of the stage (i.e. 25.4 mm full motion range). These variations also did not show notable effects.

Scanning not ideally perpendicular to the normal of the beam will result in a phase addition. This phase addition is however of no influence to the measurement as the following numerical example shows: a misalignment of 0.1 rad in the xz-plane, see Fig. 3, results in a  $\Delta z$ -displacement of 0.6 mm for a beam diameter of 6 mm. This displacement in combination with a wavelength of 75 m (i.e. c/4 MHz) of the interference signal will lead to a phase addition of  $\sim 5$  pm (i.e.  $[0.6 \text{ mm}/75 \text{ m}] \cdot 632.8 \text{ nm}$ ).

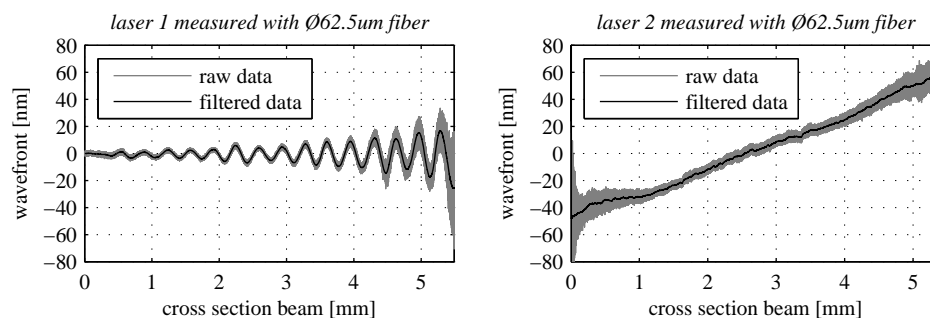


Fig. 6. Two line-scans showing the relative wavefront differences between  $f_1$  and  $f_2$ , measured with a 62.5  $\mu\text{m}$  multimode fiber scanning through the centers of the two laser beams.



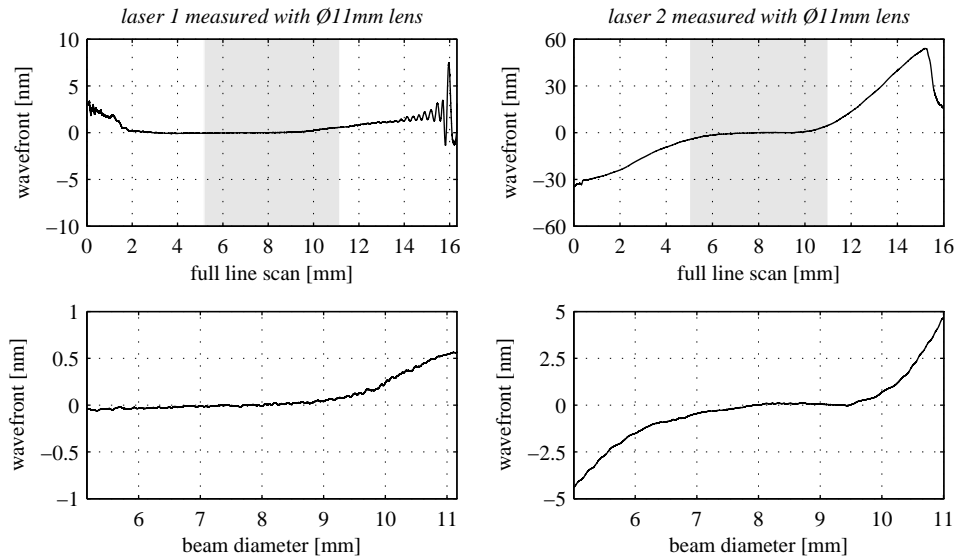


Fig. 7. The top two figures show the wavefronts from Fig. 5 but now measured using a lens with an Ø11 mm integration area. The grey areas denote the locations of the Ø6 mm coaxial beams. The two bottom figures are zoomed in on the 6 mm center parts of the two upper figures and show what is measured when using a large aperture instead of an optical fiber.

## 5. Measurement limitations and improvements

In the current setup the absolute location of the multimode fiber is not measured during scanning. Only phase-data and relative-location-data (continuous scanning velocity) of the fiber are recorded. Having no absolute position data of the fiber location requires time consuming cross correlation-methods for 3D wavefront reconstructions. Simultaneous measurement of both parameters will eliminate the need for cross-correlation between data sets and allows for improvement of the spatial resolution by applying phase deconvolution. The spatial resolution can also be improved by using smaller fiber cores (e.g. single-mode fibers), however this requires more powerful lasers or increased photodetector sensitivity.

The measured wavefront consists of the relative phase differences between the wavefronts of the two source frequencies; it is therefore a relative wavefront measurement that cannot distinguish between the wavefront shapes of the individual source frequencies.

The method presented is primarily applicable for heterodyne systems but measuring in homodyne systems is also possible. Wavefront evaluation as shown in Fig. 3 in a homodyne system only can take place after the interferometer due to the absence of a measurable beat frequency. The phase noise for a homodyne system is expected to be higher due to measuring DC irradiance instead of an AC beating signal. We might consider generating a beat frequency (i.e. a second wavefront) with an external acousto optic modulator.

Compared to other measurement systems, this system is in its current implementation relatively slow. When measuring at a rate of ~5.58 kHz one line scan required on average about ~60 seconds. After more thorough testing this could be brought back to about 15 seconds per line without notable changes in the results, see Fig. 5. As solution a ribbon fiber could be used, having multiple fibers in a row (obtaining several line scans in parallel) requiring more optical channels but will reduce scanning time considerably. Reduction of the scanning time requires further investigation in order to increase the feasibility for commercial usage.

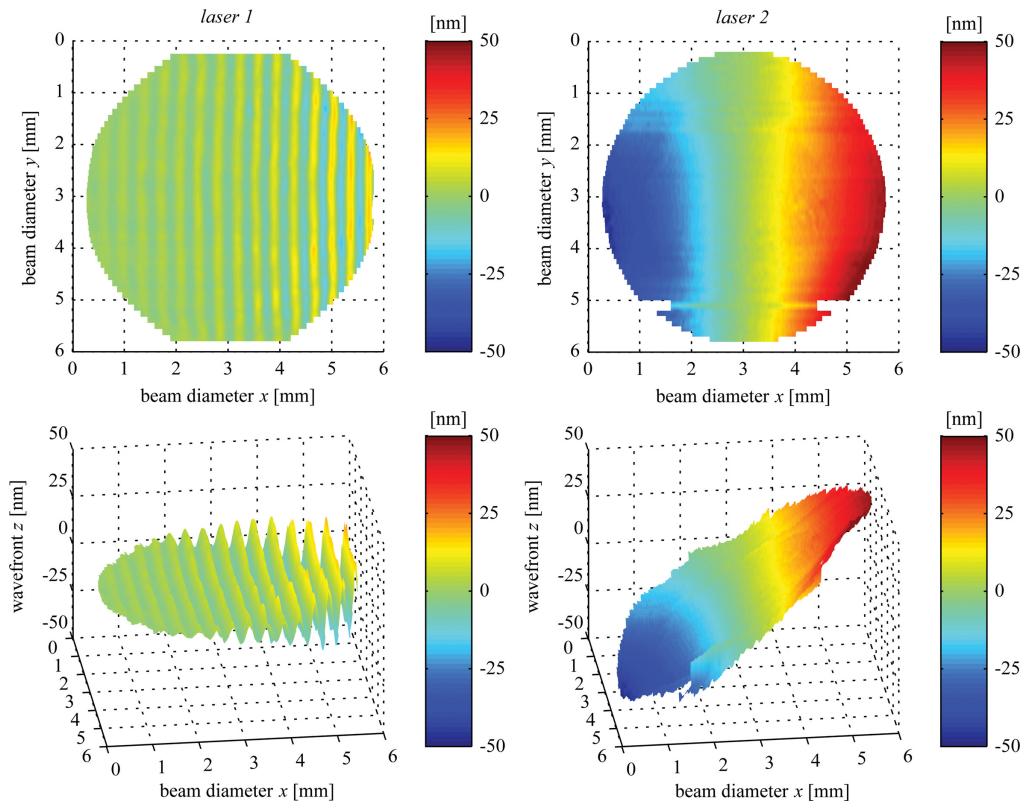


Fig. 8. 3D wavefront reconstructions build from multiple line-scans as shown in Fig. 5. The top images show front views, the bottom two images show isometric projections (see Figs. 3 and 4 for the orientation). Measurements at the top and bottom of the beam of *laser 1* showed to contain much noise and have been left away for clarity. *Laser 2* shows unexplainable behavior at  $\sim 5$  mm y-axis height that is not caused by the measurement method, multiple line scans at the same y-location showed the same outcome; therefore the laser source must be the cause.

## 6. Conclusions

In this publication a new relative optical wavefront measurement method is presented for evaluating wavefront quality related to beam walkoff behavior in displacement interferometer systems. The interference signal wavefronts of two types of coaxial heterodyne frequency laser heads were measured for demonstrating the method. The measurement method has a spatial resolution of  $62.5 \mu\text{m}$ , currently limited by the core diameter of the optical multimode detection fiber. The obtained phase resolution is shown to be in the order of  $\sim 25$  pm or  $\sim \lambda/25000$  based upon an Allan deviation analysis. The systems' repeatability has shown to be  $0.8$  nm for subsequent measurements ( $\sim 5$  min) and  $0.82$  nm with one week in-between measurements. From these numbers we can conclude that the measurement method offers high repeatability and that the laser source has a high relative wavefront stability between the source frequencies. The discussed measurement setup is thus able to operate with high spatial- and phase resolution simultaneously which can be varied by the user depending on the measurement time available without the need to replace hardware.

The method requires no (expensive) dedicated measurement equipment; it uses standard commercial optics and operates with the same phase measurement equipment as is normally used for heterodyne displacement interferometry. For the current setup a coaxial heterodyne beam suffices for performing the measurement, no optical flats or reference wavefronts are needed. The coaxial beam makes it also possible to perform measurements in air and to use

low cost optical components thanks to optical pathway overlap of the two source frequencies, both beams are equally affected by phase inducing disturbances. The applied components allow for compact design making it overall an easy to implement and useful tool for inspecting wavefront quality and beam walkoff behavior within existing interferometer systems.

The presented measurement method might not beat state-of-the-art dedicated tools in either the spatial- or phase resolution regime alone, it does offer high performance in both regimes simultaneously.

Follow up research is planned to investigate individual wavefronts (absolute wavefront measurements), wavefront evaluation after a heterodyne interferometer and the implementation in a homodyne system.

### **Acknowledgments**

This work was supported by the Dutch IOP (IPT04001) in the Netherlands. The authors are thankful for the support by Agilent Technologies and the VSL Dutch Metrology Institute, for providing equipment used during this research. The authors would also like to thank the reviewers for aiding in explaining the measurement method in a clear way.